nature communications

Article

https://doi.org/10.1038/s41467-025-63904-2

High-strength, multi-mode processable bamboo molecular bioplastic enabled by solvent-shaping regulation

Received: 14 March 2025

Accepted: 29 August 2025

Published online: 07 October 2025

Check for updates

Hongying Tang[1], Zhihan Tong[1], Rui Zhang[1], Xiaona Li[1], Suqing Zeng[1] ✉, Dawei Zhao[1,2] ✉ & Haipeng Yu[1] ✉

The global reliance on petrochemical plastics has led to severe environmental crises, necessitating sustainable alternatives that combine high performance with circularity. While bioplastics derived from biomass show promise, their widespread adoption is hindered by inferior mechanical properties, limited processability, and reliance on food-competing feedstocks. Here, we present a molecular engineering strategy to fabricate high-strength bamboo molecular plastics (BM-plastics) through a solvent-regulated shaping process. By employing deep eutectic solvents to disassemble bamboo cellulose's hydrogen-bond network and ethanol-mediated molecular stimulation to reconstruct dense hydrogen-bond interactions, we achieve a bioplastic with exceptional mechanical strength (tensile strength: 110 MPa, flexural modulus: 6.41 GPa), thermal stability (>180 °C), and versatile processability via injection, molding, and machining techniques. The BM-plastic outperforms most commercial plastics and bioplastics in mechanical and thermo-mechanical metrics while maintaining full biodegradability in soil within 50 days and closed-loop recyclability with 90% retained strength. Techno-economic analysis confirms its cost competitiveness, bridging the gap between sustainability and industrial scalability. This work establishes a method for transforming abundant bamboo cellulose into high-performance, eco-friendly materials, offering a viable pathway to mitigate plastic pollution and fossil resource dependence.

The ubiquity of petrochemical plastics in modern society, evident in packaging, construction, and electronics, is underpinned by their low cost, durability, and processability[1–3]. Since the 1950s, global plastic production has surged exponentially, with projections indicating a staggering output of 1.23 billion tons by 2060 (Fig. 1a)[4–7]. Yet, the environmental toll of this reliance is catastrophic: less than 10% of plastics are recycled, while the remainder accumulates in landfills and oceans, fragmenting into persistent microplastics that infiltrate ecosystems and food chains[8–13]. This crisis underscores an urgent need for sustainable materials that reconcile industrial utility with environmental safety.

Bioplastics derived from renewable biomass, such as polylactic acid (PLA) and polyhydroxyalkanoate (PHA), have emerged as alternatives. However, their adoption remains constrained by critical limitations. Starch-based bioplastics compete with food crops for feedstocks[14], while PHA production relies on costly fermentation processes and petrochemical inputs[15,16]. Furthermore, most bioplastics exhibit inadequate mechanical strength, thermal stability, and

[1]Key Laboratory of Bio-based Material Science and Technology of Ministry of Education, Northeast Forestry University, Harbin, PR China. [2]Key Laboratory on Resources Chemicals and Materials of Ministry of Education, Shenyang University of Chemical Technology, Shenyang, PR China.
✉e-mail: zengsuqing@nefu.edu.cn; daweizhao@syuct.edu.cn; yuhaipeng20000@nefu.edu.cn

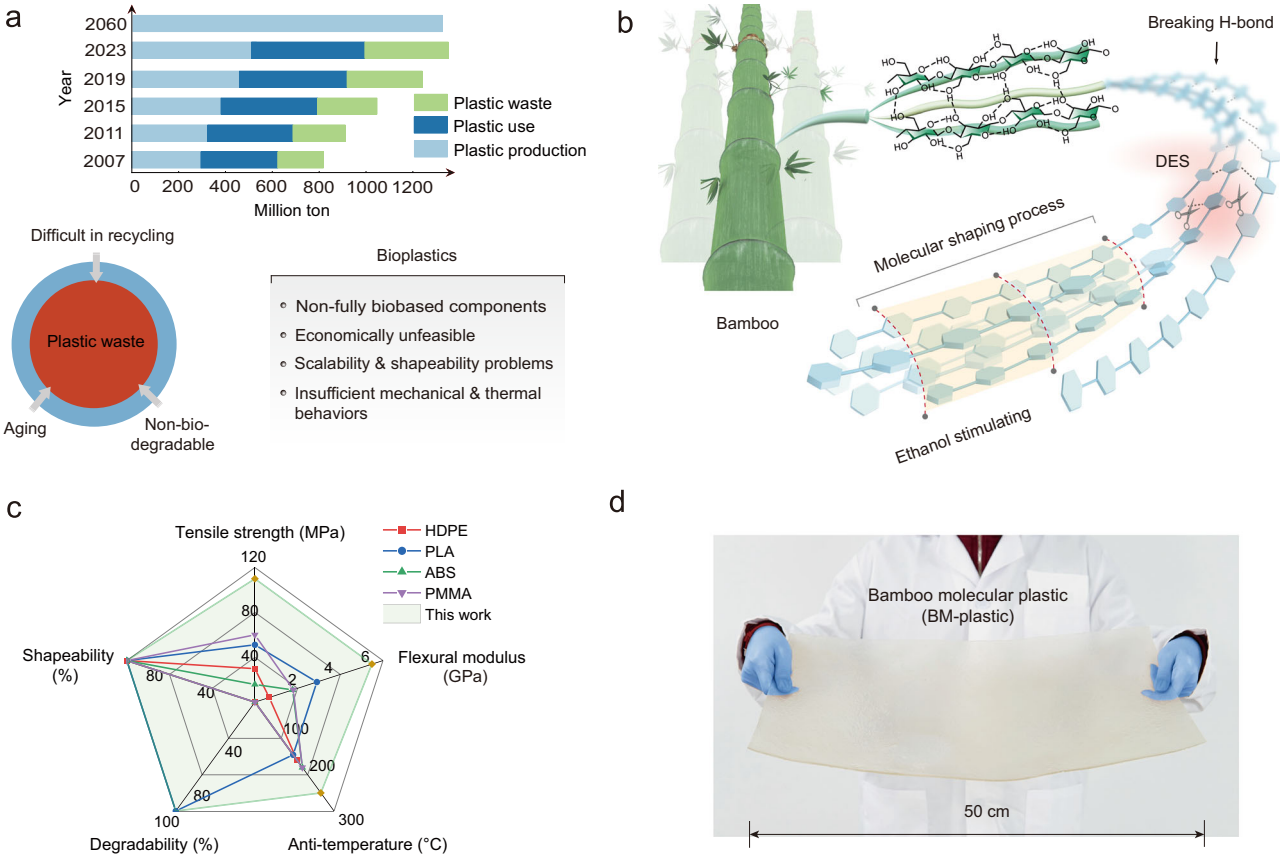

Fig. 1 | Conceptual scheme of the development of BM-plastic via molecular shaping process. a Histogram of global plastic production, use, and waste from 2007 to 2060. The bottom left illustrates the deficiencies associated with plastic waste, while the bottom right outlines the aspects in which current bioplastics require enhancement. **b** Schematic diagram of molecular shaping design for the construction of BM-plastic through DES treatment and ethanol molecular stimulation. Each element of Schematic diagram was conceived by the authors of this work and drawn using Adobe Photoshop CC 2019 and 3ds Max 2018 software. **c** Radar plot of BM-plastic and commercial plastic (HDPE, PLA, ABS and PMMA). **d** Demonstration of the large-scale preparation of BM-plastic.

processability compared to conventional plastics, hindering their use in demanding applications like automotive or infrastructure[17]. These challenges highlight a pressing scientific gap: how to transform abundant, non-food biomass into high-performance materials that match or exceed the functional properties of petrochemical plastics while enabling circularity.

Bamboo, a rapidly growing lignocellulosic resource, yields up to 78.3 tons per hectare—4.5 times more than traditional timber—making it a scalable and sustainable feedstock. Recent efforts to fabricate bamboo-based plastics through cellulose extraction and hot-pressing have achieved partial success (Supplementary Table 1), fully demonstrating the exceptional mechanical properties of bamboo fibers, yet the resulting materials suffer from brittleness (elongation rate ≤ 5%), limited moldability, and insufficient mechanical robustness[18–21]. A fundamental bottleneck lies in the hierarchical structure of native cellulose, where rigid hydrogen-bond (H-bond) networks restrict molecular mobility and interfacial interactions, impeding effective shaping and performance optimization. Addressing this requires innovative strategies to deconstruct and reconfigure cellulose at the molecular level while retaining its intrinsic strength.

Here, we propose a solvent-mediated molecular engineering strategy to fabricate high-performance bamboo molecular plastics (BM-plastics) with tunable H-bond networks. By employing a hydrated $ZnCl_2$/formic acid deep eutectic solvent (DES), we disassemble the native H-bond matrix of bamboo cellulose into a homogeneous molecular system. Subsequent ethanol stimulation triggers the rearrangement of cellulose chains, fostering dense, ordered H-bond interactions between hydroxyl and formate ester groups (Fig. 1b). This dual-step process not only overcomes the trade-off between mechanical strength and processability (Fig. 1c) but also enables scalable manufacturing under ambient conditions (Fig. 1d). In contrast to traditional processing methods that often require toxic or costly reagents and are associated with high energy consumption, our solvent-mediated molecular engineering approach delivers substantial operational advantages while significantly improving the performance characteristics of the resulting BM-plastic (Supplementary Table 2). The resultant BM-plastics demonstrate impressive mechanical properties and impressive thermal stability above 180 °C, exceeding the properties of high-density polyethylene (HDPE), acrylonitrile butadiene styrene (ABS), and commercial bioplastics such as PLA (Fig. 1c)[22–25]. Beyond performance, the BM-plastic embodies circularity: it is fully biodegradable in soil within 50 days and retain 90% of their mechanical properties after recycling. A techno-economic analysis further confirms their cost competitiveness, bridging the gap between sustainability and industrial feasibility. By leveraging bamboo's abundance and a low-energy processing route, this work establishes an approach for transforming lignocellulosic biomass into next-generation materials. The implications span multiple sectors, from automotive components to construction panels, presenting a viable pathway to decouple material production from fossil resources and address the plastic pollution crisis.

Results

Fabrication and performance of BM-plastic

A hydrated $ZnCl_2$/formic acid solution was synthesized to disrupt the native H-bond network of bamboo cellulose and convert the fibers into

a homogeneous cellulose molecular system at room temperature (Supplementary Fig. 1). In this process, some hydroxyl groups (-OH) in the cellulose underwent esterification with formic acid, introducing formate ester groups (-OCHO) into the cellulose structure with a degree of substitution (DS) of 0.4. From the Fourier transform infrared spectroscopy (FTIR), we clearly observe the characteristic C = O stretching peak at a wavenumber of 1710 cm^{-1} (Supplementary Fig. 2). This esterification of -OH in cellulose is beneficial for the construction of dense molecular networks (Fig. 2a) and the improvement of the material's mechanical properties. Addition of a calcium chloride solution then led to the formation of a bamboo molecular hydrogel (denoted BM-gel), characterized by the reformation of H-bond networks among cellulose chains and water molecules. The mechanical tensile properties of BM-gels with different cellulose concentrations were compared. A BM-gel with water content of 82.7 ± 0.5 wt% prepared from a 7 wt% cellulose solution exhibits a remarkable tensile strength of 9.65 MPa (Supplementary Fig. 3), which exceeds that of previously reported cellulose-based gel materials[26–29]. This finding underscores the potential use of BM-gel in the development and fabrication of bio-based plastics.

Subsequent treatment of BM-gel with ethanol disrupted the H-bonds between cellulose molecules and water, enabling tighter packing of the cellulose chains and enhancing H-bonding between -OH and -OCHO groups. This treatment resulted in the formation of a densely packed, structurally enhanced BM-plastic. Mechanical tests illustrated that ethanol-treated BM-gel exhibited significantly improved rigidity and toughness compared to untreated sections (Fig. 2b). X-ray diffraction (XRD) analysis showed a transformation in the structural domains from a broad, disordered peak at $2\theta = 28°$ in BM-gel to distinct crystalline peaks at $2\theta = 12.1°$ and 18.8° in the BM-plastic, indicative of the transformation to a cellulose II structure (Fig. 2c). Additionally, the analysis of small-angle X-ray scattering (SAXS) curves revealed the disappearance of a scattering peak at $q = 0.21\ nm^{-1}$ in BM-plastic, confirming the dense and ordered nature of the structural domains when compared to BM-gel (Fig. 2d).

These findings demonstrate that the introduction of ethanol not only restructures the H-bonding among cellulose molecules but also promotes their self-assembly, leading to the formation of denser and more ordered structural morphologies in BM-plastic. A comparison of scanning electron microscopy (SEM) images between BM-gel and BM-plastic shows a significantly denser and more coherent microstructure in the BM-plastic, with an absence of pores (Fig. 2e and Supplementary Fig. 4). Additionally, two-dimensional (2D) small-angle X-ray scattering (SAXS) patterns (Fig. 2f) and two-dimensional wide-angle X-ray scattering (WAXS) patterns (Fig. 2g) reveal that BM-plastic displays more intense 2D ring patterns compared to BM-gel, indicative of periodic structures and oriented domains. These structural features are likely to enhance the mechanical properties and moldability of BM-plastic, as shown in physical verification experiments where BM-plastic successfully lifted a 2 kg weight and withstood a load of 200 g (Supplementary Fig. 5).

Mechanical properties and dimensional stability

The mechanical properties of BM-plastic were comprehensively evaluated, encompassing tensile strength, flexural strength, toughness, and hardness. Analysis of the tensile stress-strain curves (Fig. 3a) reveals that BM-plastic exhibits a strain limit of no more than 5% at stresses exceeding 60 MPa, underscoring its rigid behavior. As tensile stress increases, the material shows notable extensibility and toughness, with plastic deformation accounting for over 90% of its total elongation. Notably, BM-plastic achieves an ultimate tensile strength of 110 MPa, a substantial increase from the 9.7 MPa of BM-gel, and a dramatic rise in Young's modulus from 1.7 MPa to 2.2 GPa, an increase of over 1290-fold (Fig. 3b). Even when compared to dried BM-gel (Supplementary Fig. 6a), BM-plastic still exhibits high mechanical properties, measuring tensile strength of 1.1 times and elastic modulus of 1.4 times greater, respectively, than those of the dried BM-gel. This exceptional mechanical feature is attributed to the formation of enhanced H-bonding in BM-plastic (Supplementary Fig. 6b). Meanwhile, in comparison to the plastic lacking Ca^{2+} ion treatment, BM-plastic demonstrates impressive mechanical properties, with its tensile strength being up to eight times greater than that of the untreated plastic (Supplementary Fig. 7). These enhancements mark a significant improvement over previously characterized cellulose-based plastics and composites[30–33], making BM-plastic a strong candidate for applications in sectors like household products, automotive parts, and public facilities.

In bending tests, BM-plastic demonstrates strong resistance to deformation, maintaining a plateau of plastic deformation with an ultimate flexural strength of 92 MPa—markedly higher than the 0.08 MPa recorded for BM-gel (Fig. 3c, d). The flexural Young's modulus reaches 6.41 GPa, over 3330 times that of BM-gel (1.87 MPa), highlighting its capacity to withstand substantial bending without becoming brittle. Nanoindentation tests further reveal that the hardness of BM-plastic is five times greater than that of BM-gel (Fig. 3e).

Thermogravimetric (TG) analysis, dynamic mechanical analysis (DMA), and dimensional analysis in extreme conditions were conducted to assess the thermal performance and structural stability of BM-plastic. Compared to BM-gel, the ethanol-derived BM-plastic exhibits enhanced resistance to temperatures exceeding 250 °C (Supplementary Fig. 8). The storage modulus (G') and loss modulus (G'') remained relatively stable from 25 to 250 °C, indicating impressive structural stability (Fig. 3f). In contrast, both moduli of BM-gel showed significant increases after 100 °C, implying substantial deformation and solidification.

Dimensional stability tests at high and low temperatures (Fig. 3g, i) over a 7-day period at 100 °C and −30 °C demonstrate that BM-plastic preserves its mechanical integrity, allowing for significant twisting and bending without fracture. The dimensional stability across a temperature range of −30 to 100 °C is impressive (Fig. 3h). Additionally, the resistance of BM-plastic to moisture and various organic solvents is evaluated. After exposure to 70% relative humidity (RH) for 30 days, BM-plastic maintains its original structure with minimal volume change (Fig. 3i). Corrosion resistance tests involving dichloromethane, tetrahydrofuran, methanol, sulfuric acid solution (pH 1, 0.05 mol/L), and sodium hydroxide solution (pH 13, 0.1 mol/L) over a 7-day period demonstrate that BM-plastic retains its shape and physical integrity without swelling, collapsing, or disintegrating (Supplementary Fig. 9). These robust properties highlight BM-plastic's potential for use in the manufacturing of durable containers and various engineered products, demonstrating its versatility and resilience under challenging conditions.

Comparison of BM-plastic with commercial plastics

To effectively demonstrate the advantages of BM-plastic, we performed a comprehensive comparative analysis with conventional petrochemical plastics. The tensile stress-strain curves highlighted in Fig. 4a reveal that BM-plastic exhibits a distinct yield plateau indicating impressive rigidity and malleability at elevated mechanical performance levels. Compared to widely-used commercial plastics such as ABS, high impact polystyrene (HIPS), polyamide (PA66), PMMA, and PLA, BM-plastic offers considerably higher tensile strength, Young's modulus, flexural strength, and flexural modulus—registering at 103.77 MPa, 2.24 GPa, 97.27 MPa, and 6.41 GPa, respectively (Fig. 4b and Supplementary Table 3). Additionally, BM-plastic achieves a notable work of fracture of 80 kJ m^{-3} (Fig. 4c), surpassing that of both traditional commercial plastics and bioplastics outlined in refs. 34–43, thus confirming its potential for advanced engineering applications.

Maintaining dimensional and shape stability under high temperature is crucial for polymeric materials. When subjected to a

https://doi.org/10.1038/s41467-025-63904-2

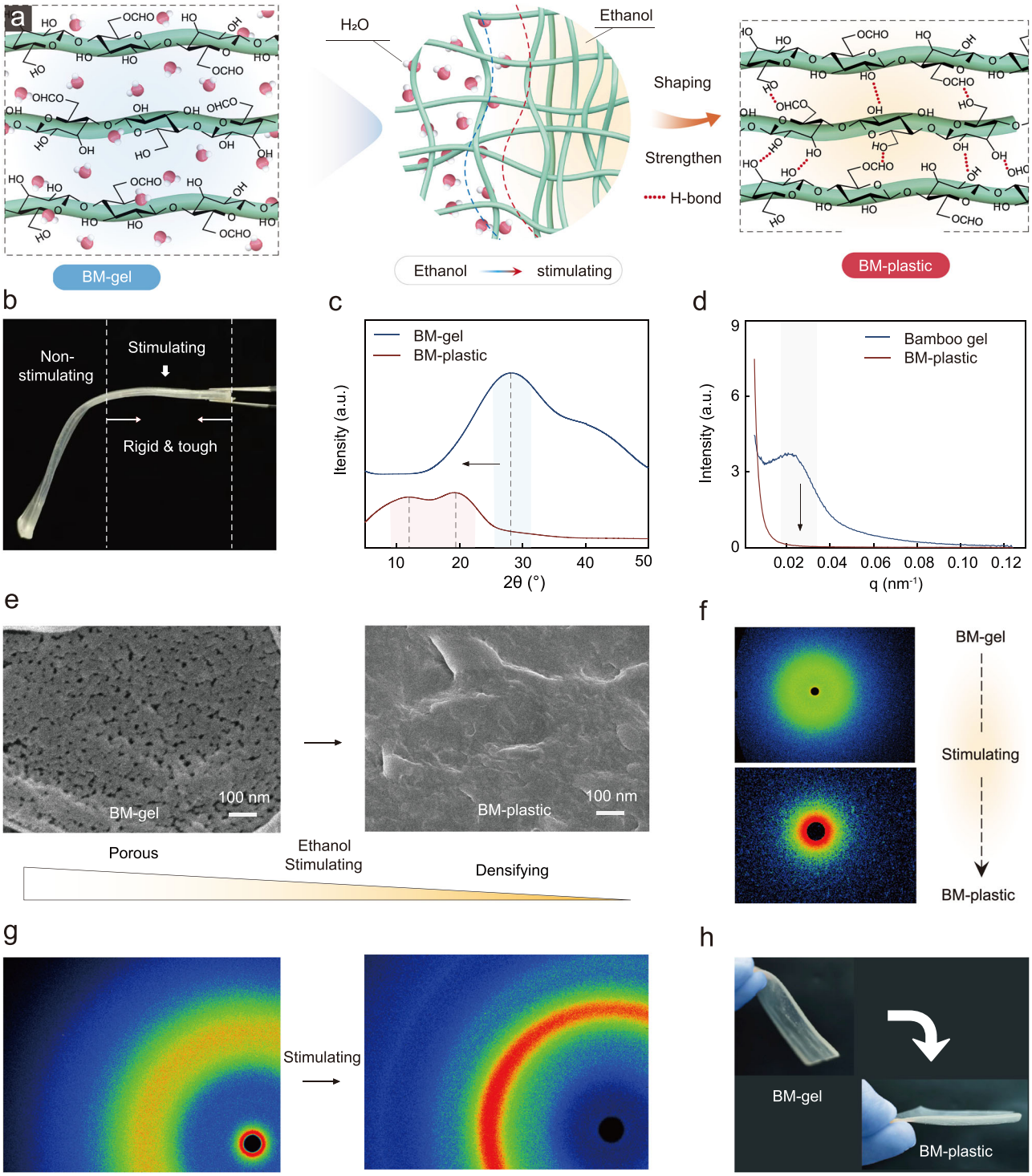

Fig. 2 | Investigating the construction mechanisms and morphological structure of BM-plastic. a Schematic procedure diagrams for the fabrication of BM-plastic. Each element of schematic procedure diagram was conceived by the authors of this work and drawn using Adobe Photoshop CC 2019 and 3ds Max 2018 software. **b** A digital photo of the BM-gel, showing the contrast between the vertical section (without ethanol stimulation) and the horizontal section (with ethanol stimulation). **c** XRD pattern of BM-gel and BM-plastic. **d** Investigating the SAXS curves of BM-gel and BM-plastic. **e** SEM images of BM-gel and BM-plastic. **f** Comparison of SAXS 2D patterns between BM-gel and BM-plastic. **g** Comparison of WAXS 2D patterns between BM-gel and BM-plastic. **h** Digital images of BM-gel with flexibility and BM-plastic with toughness and robustness.

180 °C environment for 2 h, conventional plastics like ABS, HIPS, PA66, and PMMA exhibit significant deformation and increased brittleness. In stark contrast, BM-plastic maintains exceptional structural stability and mechanical toughness, showing no deformation and supporting bending without catastrophic failure (Fig. 4d). Additional analysis of the thermo-mechanical behavior of BM-plastics through dynamic mechanical analysis (DMA) highlighted an enhanced thermal-mechanical stability with a glass transition temperature exceeding 150 °C. Even at this elevated temperature, BM-plastic still retains a mechanical modulus of approximately 3.6 GPa (Fig. 4e), a property comparable to that of HIPS, noted for its high-temperature resilience (Supplementary Fig. 10). These properties solidify BM-

https://doi.org/10.1038/s41467-025-63904-2

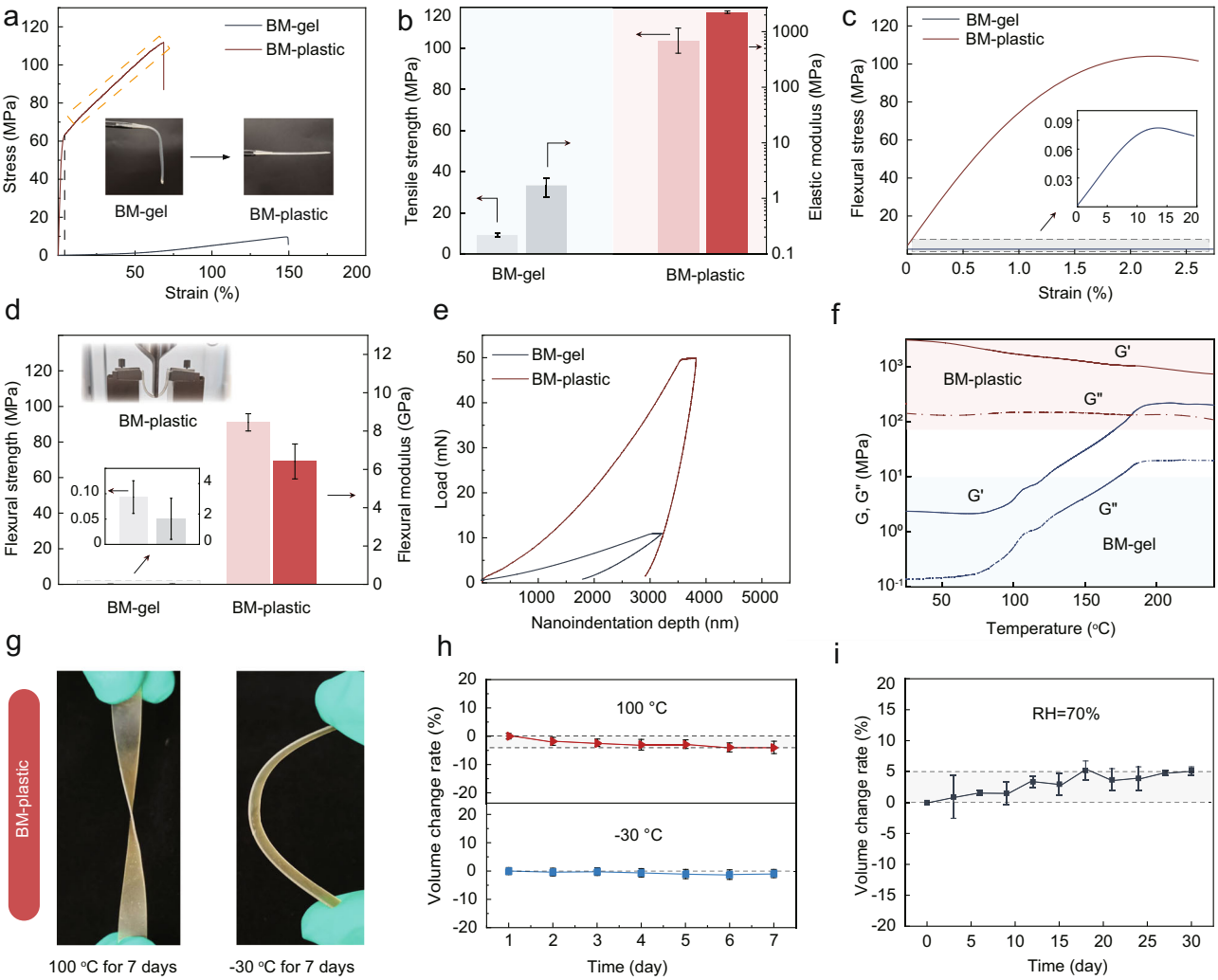

Fig. 3 | Mechanical properties and dimensional stability of BM-plastic. a Tensile stress-strain curves of BM-gel (water content 82.7 ± 0.5 wt%) and BM-plastic. Insets show the digital images of BM-gel with flexibility and BM-plastic with rigidity. **b** Comparison of the tensile strength and elastic modulus of BM-gel and BM-plastic. **c** Three-point bending stress-strain curves of BM-gel and BM-plastic. **d** Comparison of the flexural strength and elastic modulus of BM-gel and BM-plastic. Insets show the digital images of BM-plastic with good toughness during three-point flexural test. **e** Load–displacement curves for static nanoindentation tests of BM-gel and BM-plastic. **f** Investigating the DMA behavior of BM-gel and BM-plastic. **g** Digital images of BM-plastic, showing good mechanical integrity when treated at 100 °C and −30 °C for 7 days, respectively. **h** Assessment of volume changes in BM-plastic subjected to temperatures of 100 °C and −30 °C for 7 days. **i** Rate of volume change in BM-plastic under an atmospheric condition with 70% RH over 30 days. Values in (**b**, **d**, **h**, and **i**) represent their means ± SDs from $n = 5$ independent samples.

plastic's suitability for high-temperature applications in various engineering fields.

Moreover, BM-plastic exhibits a low coefficient of thermal expansion (CTE) of $40.7 \times 10^{-6} K^{-1}$ at a room temperature of 25 °C (Fig. 4f), which further underscores its exceptional dimensional stability. Along with robust mechanical features and temperature resistance, BM-plastic also displays impressive impact resistance (Fig. 4g and Supplementary Fig. 11), with an impact strength of 110 kJ/m^2. Even after being exposed to a relative humidity (RH) of 90% for 48 h and immersed in water for 24 h, BM-plastic still exhibits attractive mechanical properties, including tensile strength of 43.24 MPa and 22.85 MPa (Supplementary Fig. 12 and Supplementary Table 4). These attributes significantly enhance the usability of BM-plastics in the construction industry, providing effective mitigation against damage from external impacts.

Processing, shaping, and scalability of BM-plastic

Melt processing, encompassing techniques such as extrusion, injection, and molding, is the predominant industrial method utilized for shaping plastics. Similarly, our bamboo cellulose molecular system, characterized by its fluidity, can be molded using comparable melt-processing techniques used for commercial plastics. This facilitates the casting of the bamboo cellulose into various molds. Following this molding, we can easily produce BM-plastic in customizable three-dimensional shapes via an ethanol stimulation process. As depicted in Fig. 5a, the resulting BM-plastics are showcased in an array of shapes, including stars, shells, starfish, and gears. And it also can be molded into shapes like flowers and stars etc. (Fig. 5b). Optical characterization reveals that BM-plastic exhibits a haze value of 10.12% with a high light transmittance of 90.32% at a controlled thickness of 0.15 mm (±0.02 mm), demonstrating its potential for applications requiring balanced transparency and light diffusion (Supplementary Fig. 13).

Extending the aforementioned processing methods, BM-plastic can be shaped into large-sized products using a straightforward mechanical technique. For instance, a BM-plastic sheet measuring 50 cm in length and 35 cm in width was successfully transformed into complex structures, including two honeycomb panels and a corrugated panel as shown in Fig. 5c. Furthermore, this bamboo molecular shaping strategy can also accommodate other solvents, such as acetonitrile, acetone, and tetrahydrofuran (Supplementary Fig. 14). The

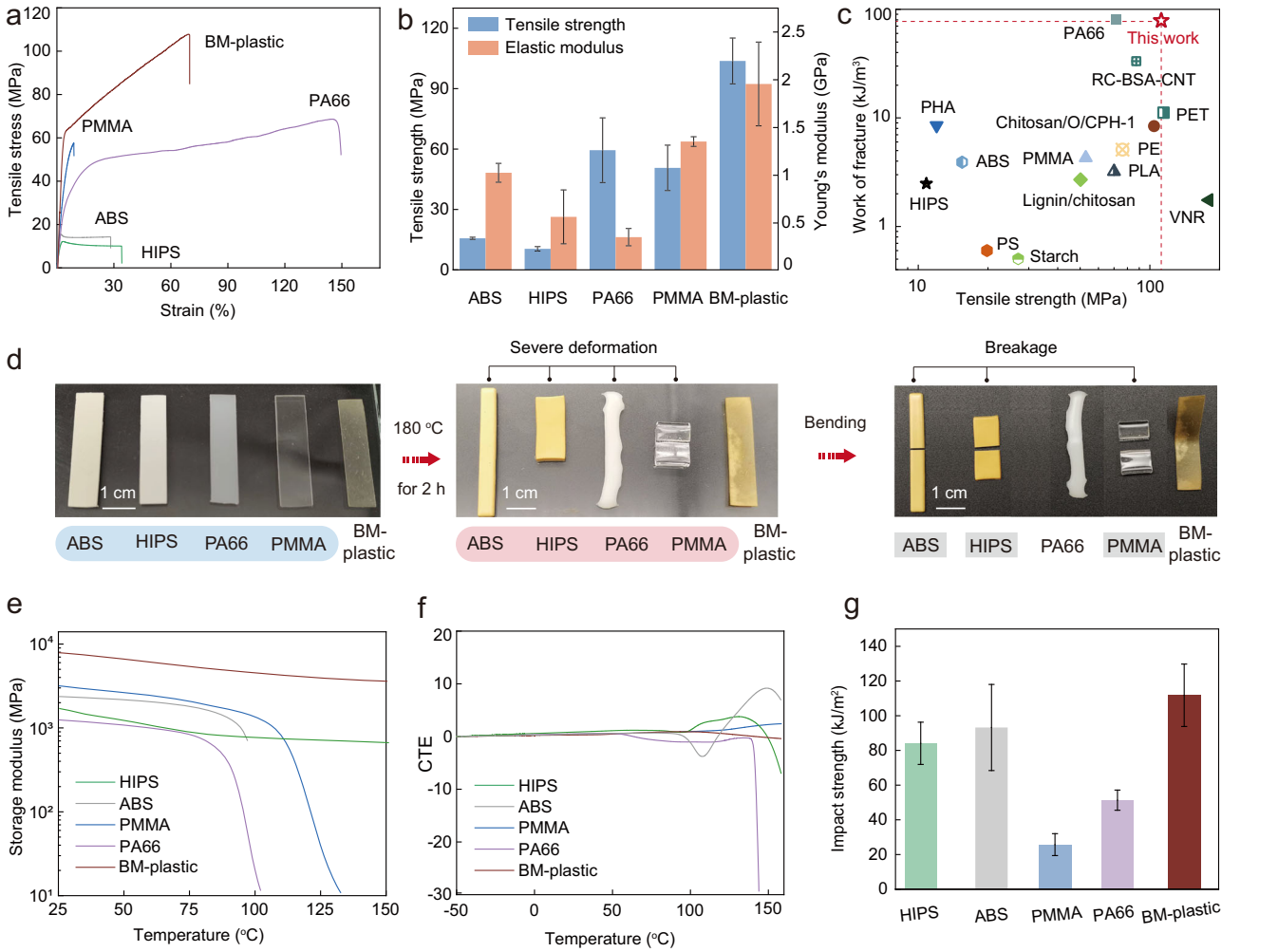

Fig. 4 | Comparison of mechanical and thermal properties of BM-plastic with commercial plastics. a Tensile stress-strain curves of ABS, HIPS, PA66, PMMA, and BM-plastic. All samples with thickness of 1.00 ± 0.01 mm. **b** Comparison of tensile strength and modulus of ABS, HIPS, PA66, PMMA, BM-plastic. **c** Investigating the tensile strength and work of fracture between BM-plastic, commercial plastics, and bioplastics. **d** Optical images from high-temperature resistance experiments conducted on BM-plastic and several commercial plastics. All samples with thickness of 1.00 ± 0.01 mm. **e** Comparison of the storage modulus between BM-plastic, ABS, HIPS, PA66, and PMMA. These curves are obtained through DMA testing. **f** Comparative analysis of dimensional change values of BM-plastic relative to plastics such as ABS, HIPS, PA66, and PMMA. **g** Comparison of impact strength between BM-plastic, ABS, HIPS, PA66, and PMMA. Values in (**b** and **g**) represent their means ± SDs from $n = 5$ independent samples.

process does not require high temperatures or high pressures and leverages the abundant availability of bamboo feedstocks. This positions BM-plastic as a scalable alternative to conventional plastics. Such processability advantages align with the principles of green manufacturing by minimizing energy consumption and reducing the environmental footprint.

Recyclability, degradability and economic feasibility

Compared to petrochemical plastics, BM-plastic is distinguished by its closed-loop recyclability, which stems from the recyclable nature of its bamboo cellulose base and the deep eutectic solvents (DES) employed in its production. As illustrated in Fig. 6a, waste BM-plastic fragments undergo a simple recycling process: (1) The fragments are dissolved to recreate a bamboo cellulose molecular system using the recycled DES solvent. (2) A calcium chloride solution is introduced to form BM-gel, which, upon interaction with ethanol, enables BM-plastic reformation. The recycled BM-plastic exhibits impressive mechanical properties, with a tensile strength of 97 MPa and an elastic modulus of 2.7 GPa (Supplementary Fig. 15), which are comparable to those of the original BM-plastic.

Environmental sustainability is further enhanced by the BM-plastic's degradability, as detailed in soil degradation studies at 25 °C. Within 50 days, our BM-plastic achieves complete morphological disintegration and biodegradation (Fig. 6b), mainly due to microbial activity. In contrast, conventional petrochemical plastics, such as ABS, HIPS, PA66, and PMMA, show negligible degradation, and other bioplastics like PLA and PBAT only partially degrade. The effective biodegradation of BM-plastic in natural soils addresses significant concerns of persistent plastic pollution and positions BM-plastic as an effective alternative for managing commercial plastic waste, promoting both environmental sustainability and resource circularity.

A techno-economic analysis (TEA) was conducted, revealing that the production cost of BM-plastic falls between that of conventional petrochemical plastics (PMMA, HIPS, and PA66) and PLA bioplastic (Fig. 6c, Supplementary Tables 5 and 6). The main cost factors for BM-plastic are the availability of raw materials and the reusability of DES solvent and ethanol, constituting 37.72% and 23.82% of total costs, respectively. With electricity costs comprising only 3.32% of total expenses, the low-energy production process is highlighted. Despite having slightly higher production costs than some plastics, BM-

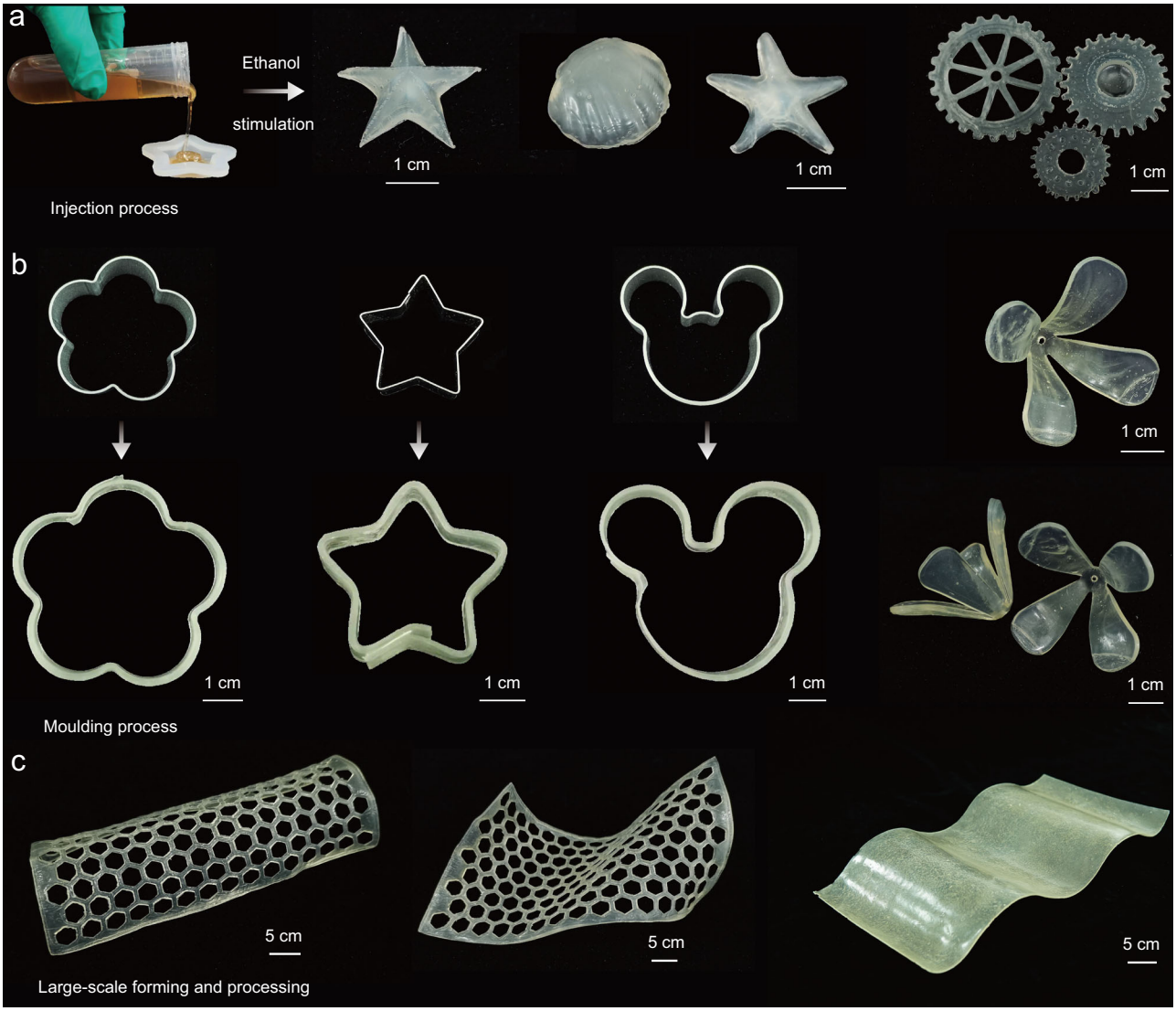

Fig. 5 | Processability and formability of BM-plastics for diverse products. **a** Illustration of the BM-plastics injection process utilized for the fabrication of stars, shells, starfish, and gears. **b** Depiction of the molding process for creating various BM-plastics products. **c** Demonstration of the large-scale forming fabrication of BM-plastics into structured products, including two honeycomb panels and a corrugated panel.

plastic's exceptional mechanical properties, thermal stability, customizable formability, and reduced environmental impact enhance its market competitiveness in the bioplastics sector.

Discussion

In this research, we introduce a sustainable and scalable approach for producing high-performance bioplastic from bamboo cellulose utilizing an ethanol-assisted molecular shaping process. The resulting BM-plastic demonstrates robust mechanical properties, with tensile strength exceeding 100 MPa, flexural modulus surpassing 6 GPa, and thermal stability above 180 °C—properties that outperform those of conventional plastics such as PE, ABS, and PMMA, as well as PLA bioplastic. The ethanol shaping technique facilitates the scalable and large-scale fabrication of bioplastic products with intricate 3D geometries under ambient conditions, compatible with conventional manufacturing processes like injection molding and machining.

Moreover, BM-plastic showcases impressive closed-loop recyclability, retaining 90% of its original mechanical strength after reprocessing. It also achieves complete biodegradation in natural soil conditions within 50 days, effectively addressing the issues of resource circularity and environmental persistence. Economically, the production costs of BM-plastic are competitive at $2302.03 per ton. Collectively, these economic benefits, combined with its impressive mechanical properties, versatility in shaping, high thermal resistance, and environmentally friendly attributes of recyclability and biodegradability, establish BM-plastic as a viable sustainable alternative to non-degradable plastics.

Methods

Materials

Bamboo stems, zinc chloride ($ZnCl_2$), calcium chloride ($CaCl_2$), hydrogen peroxide (H_2O_2) and anhydrous ethanol were purchased from Aladdin (China). Formic acid (FA), dichloromethane (DCM), tetrahydrofuran (THF), methanol (MeOH), acetonitrile, and acetone were purchased from Fuyu Chemical (China). Sulfuric acid was purchased from Tianjin Kemiou Chemical Reagent Co., Ltd.

Preparation of bamboo cellulose

The bamboo chips were delignified using a 10 v/v% peroxyformic acid solution at 50 °C for 12 h, and neutralized with 0.5 wt% sodium hydroxide solution for 5–10 min and washing in deionized water several times to remove the chemicals, as well as to detach the parenchymal cells from the cellulose macrofibres and dried at room

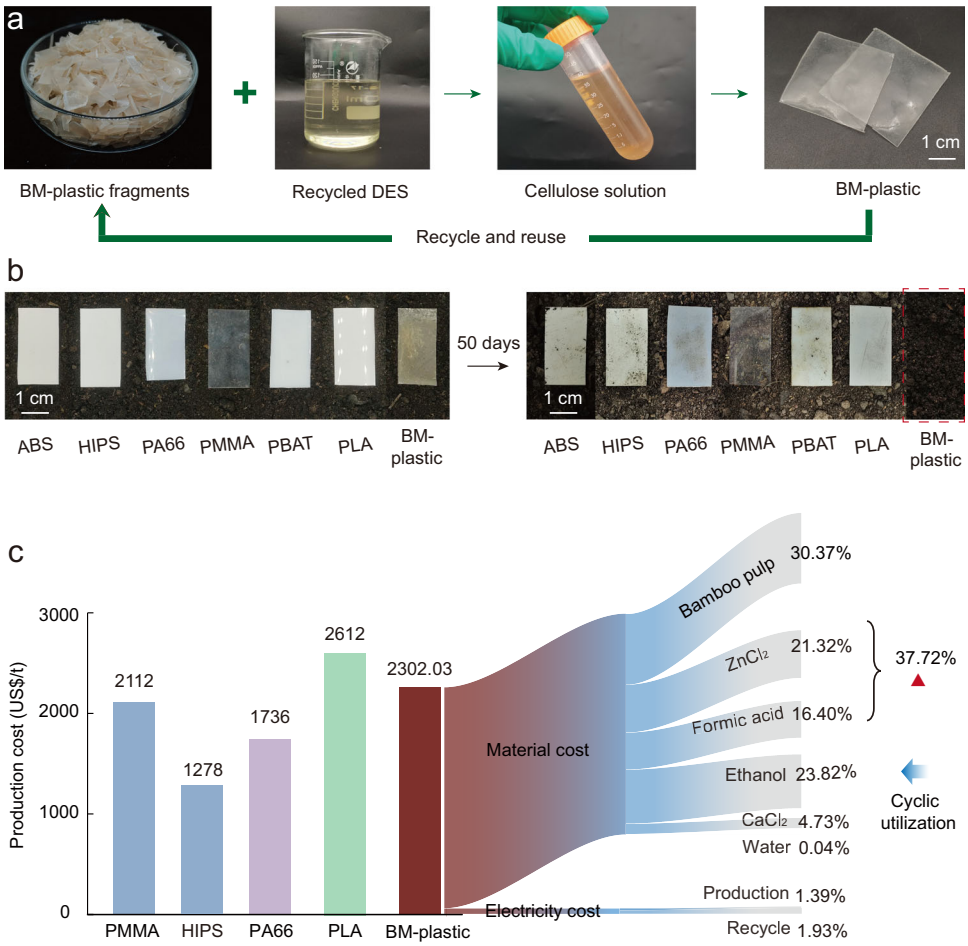

Fig. 6 | Recyclability, biodegradability, and economic feasibility of BM-plastic. a Investigating the recyclability of BM-plastic. **b** The biodegradability tests of BM-plastic and commercial plastics under natural soil. **c** Comparison of production costs of BM-plastic and commercial plastics including PMMA, HIPS, PA66, and PLA.

temperature. In this work, the peroxyformic acid solution, comprising 1 wt% sulfuric acid, is synthesized from a mixture of 30% hydrogen peroxide and formic acid at a molar ratio of 1:1.

Preparation of bamboo cellulose molecular system

Bamboo cellulose dissolution experiments were initiated by adding a specific mass of cellulose (4 ~ 8 wt%) to a $ZnCl_2$/FA ($ZnCl_2$, FA and deionized water at mole ratio of 1:2:2) solution under stirring at room temperature. Subsequently, after 1.5 h of mechanical stirring, a viscous bamboo cellulose molecular system was obtained. The DP of cellulose in the molecular system is around 730.

Preparation of BM-gel

A suitable amount of the bamboo cellulose molecular system was taken out and spread onto a smooth glass plate. Then, after soaking it in calcium chloride solution (48 wt%) for over 2 h, a flexible bamboo cellulose molecular hydrogel (denoted as BM-gel) was obtained.

Construction of BM-plastic

BM-gel was rinsed with distilled water to eliminate calcium ions and other contaminants. Then, the BM-gel was immersed in an anhydrous ethanol solution for stimulation treatment over a period of 12 h. Following this induction process, the BM-plastic can be obtained and left in open air for 12 h to facilitate the evaporation of ethanol.

Casting process of BM-plastic

The dissolved bamboo cellulose solution was poured into the corresponding mold, and immersed it in aqueous calcium chloride solution (for over 2 h) or the calcium chloride solution was poured onto the surface of cellulose solution to regenerate of the cellulose solution into a BM-gel. After the BM-gel was washed with deionized water to remove DES, the gel was stimulated in ethanol, then dried it to obtain plastic in the shape of the mold.

Molding process of BM-plastic

The BM-gel, produced in earlier steps, was positioned in the designated mold and then submerged in an ethanol solution for 12 h. Following this immersion, the gel was air-dried at room temperature for another 12 h to yield a bioplastic shaped according to the mold.

Dimensional stability tests of BM-plastic

For the high/low temperature environment, these BM-plastics with 30 × 30 × 2 mm were placed separately in a vacuum drying oven (100 °C) and a refrigerator (−30 °C) for high/low temperature dimensional stability testing. The dimensions of the samples were measured every 24 h, repeating five times. The volume change rate (V_c) is calculated through the following equation:

$$Vc = (V - V_t) \times 100\%/V \quad (1)$$

where V represents the original volume of samples, V_t represents the volume of samples at respective exposure time.

For the high humidity environment, these BM-plastics with 30 × 30 × 2 mm were placed in a constant temperature and relative humidity chamber (25 °C, 70% RH) for dimensional stability testing. The dimensions were measured every 3 d, repeating five times. The

volume change rate (V_c) was calculated through the following equation:

$$Vc = (V - V_t) \times 100\%/V \quad (2)$$

where V represents the original volume of samples, V_t represents the volume of samples at respective exposure time.

DES recycling

The spent calcium chloride solution and the ethanol used for washing the gel were collected and mixed. An equimolar amount of 48 wt% sulfuric acid was then added to precipitate the calcium ions. This mixture underwent vacuum filtration to remove the precipitated ions, followed by rotary evaporation of the residual liquid to eliminate the ethanol and recover the recycled DES.

Recycling and reuse process of BM-plastic

The recycled DES solvent ($ZnCl_2$/FA) was obtained by adding equimolar mass of sulfuric acid to precipitating $CaCl_2$, and steaming out ethanol. The recycled BM-plastic was prepared from Re-DES and BM-plastic chips, through the molecular system and molecular gel preparation process mentioned above, as well as the ethanol stimulation process. The DP of cellulose in recycled BM-plastic is around 424.

Biodegradability test

To assess the biodegradability of various materials including ABS, HIPS, PA66, PMMA, PLA, PBAT, and our BM-plastic, samples were prepared with dimensions of 40 × 20 × 1 mm and subsequently buried at a depth of 6 cm in natural soil. Periodically, these specimens were retrieved for evaluation, and their morphological alterations were recorded utilizing digital photography.

Data availability

The data supporting the findings of this work are available within the article and its supplementary files. All data are available from the corresponding author upon request.

References

1. Geyer, R., Jambeck, J. R. & Law, K. L. Production, use, and fate of all plastics ever made. *Sci. Adv.* **3**, e1700782 (2017).
2. Wang, J., Emmerich, L., Wu, J., Vana, P. & Zhang, K. Hydroplastic polymers as eco-friendly hydrosetting plastics. *Nat. Sustain.* **4**, 877–883 (2021).
3. Chen, S. et al. Robust solvatochromic gels for self-defensive smart windows. *Adv. Funct. Mater.* **33**, 2214382 (2023).
4. Jambeck, J. R. et al. Plastic waste inputs from land into the ocean. *Science* **347**, 768–771 (2015).
5. OECD. *Global Plastics Outlook: Policy Scenarios to 2060* (OECD Publishing, Paris, 2022).
6. Sardon, H. & Dove, A. P. Plastics recycling with a difference. *Science* **360**, 380–381 (2018).
7. Tian, W. et al. Microplastic materials in the environment: problem and strategical solutions. *Prog. Mater. Sci.* **132**, 101035 (2023).
8. Rochman, C. M. et al. Classify plastic waste as hazardous. *Nature* **494**, 169–171 (2013).
9. Lau, W. W. Y. et al. Evaluating scenarios toward zero plastic pollution. *Science* **369**, 1455–1461 (2020).
10. Wu, Y. et al. Revivable self-assembled supramolecular biomass fibrous framework for efficient microplastic removal. *Sci. Adv.* **10**, eadn8662 (2024).
11. Pabortsava, K. & Lampitt, R. S. High concentrations of plastic hidden beneath the surface of the Atlantic Ocean. *Nat. Commun.* **11**, 4073 (2020).
12. MacLeod, M., Arp, H. P. H., Tekman, M. B. & Jahnke, A. The global threat from plastic pollution. *Science* **373**, 61–65 (2021).
13. Amaral-Zettler, L. A., Zettler, E. R. & Mincer, T. J. Ecology of the plastisphere. *Nat. Rev. Microbiol.* **18**, 139–151 (2020).
14. Tan, C., Tao, F. & Xu, P. Direct carbon capture for the production of high-performance biodegradable plastics by cyanobacterial cell factories. *Green. Chem.* **24**, 4470–4483 (2022).
15. Koller, M. et al. Potential of various archae- and eubacterial strains as industrial polyhydroxyalkanoate producers from whey. *Macromol. Biosci.* **7**, 218–226 (2007).
16. Simon, N. et al. A binding global agreement to address the life cycle of plastics. *Science* **373**, 43–47 (2021).
17. Cui, L. et al. A strong, biodegradable, and closed-loop recyclable bamboo-based plastic substitute enabled by polyimine covalent adaptable networks. *Chem. Eng. J.* **477**, 146952 (2023).
18. Chen, C. et al. Biodegradable liquid slow-release mulch film based on bamboo residue for selenium-enriched crop cultivation. *Research* **8**, 0685 (2025).
19. Guo, D. et al. Conversion of bamboo into strong, waterproof, and biodegradable thermosetting plastic through cell wall structure directed manipulation. *ACS Nano* **18**, 24414–24425 (2024).
20. Song, W., Zhang, S., Fei, B. & Zhao, R. Mussel-inspired polydopamine modification of bamboo flour for superior interfacial compatibility of bamboo plastic composites: influence of oxidant type. *Cellulose* **28**, 8567–8580 (2021).
21. Xu, X., Xu, P., Zhu, J., Li, H. & Xiong, Z. Bamboo construction materials: carbon storage and potential to reduce associated CO_2 emissions. *Sci. Total Environ.* **814**, 152697 (2022).
22. Cao, Z. et al. Synthesis and characterization of high density polyethylene/peat ash composites. *Compos. Part B-Eng.* **94**, 312–321 (2016).
23. Akash, N. M. et al. Development of asphaltene-derived carbon fiber reinforced composites via additive manufacturing. *Carbon* **228**, 119413 (2024).
24. Behera, K., Chen, J.-F., Yang, J.-M., Chang, Y.-H. & Chiu, F.-C. Evident improvement in burning anti-dripping performance, ductility and electrical conductivity of PLA/PVDF/PMMA ternary blend-based nanocomposites with additions of carbon nanotubes and organoclay. *Compos. Part B-Eng.* **248**, 110371 (2023).
25. Scaffaro, R., Lopresti, F. & Botta, L. PLA based biocomposites reinforced with posidonia oceanica leaves. *Compos. Part B-Eng.* **139**, 1–11 (2018).
26. Jiang, H. et al. Mechanically robust, highly conductive, wide-voltage cellulose ionogels enabled by molecular network reconstruction. *Adv. Funct. Mater.* **35**, 2503512 (2025).
27. Zhu, Y. et al. A general strategy for synthesizing biomacromolecular ionogel membranes via solvent-induced self-assembly. *Nat. Synth.* **2**, 864–872 (2023).
28. Long, Q., Jiang, G., Zhou, J., Zhao, D. & Yu, H. A cellulose ionogel with rubber-like stretchability for low-grade heat harvesting. *Research* **7**, 0533 (2024).
29. Li, X. et al. Stimulation-reinforced cellulose–protein ionogels with superior mechanical strength and temperature resistance. *Adv. Funct. Mater.* **34**, 2408160 (2024).
30. Cheng, W. et al. Sustainable cellulose and its derivatives for promising biomedical applications. *Prog. Mater. Sci.* **138**, 101152 (2023).
31. Zhao, D. et al. A Stiffness-switchable, biomimetic smart material enabled by supramolecular reconfiguration. *Adv. Mater.* **34**, 2107857 (2022).
32. Xia, Q. et al. A strong, biodegradable and recyclable lignocellulosic bioplastic. *Nat. Sustain.* **4**, 627–635 (2021).
33. Zhou, G. et al. A biodegradable, waterproof, and thermally processable cellulosic bioplastic enabled by dynamic covalent modification. *Adv. Mater.* **35**, 2301398 (2023).

34. Hosoda, N., Tsujimoto, T. & Uyama, H. Green composite of poly(3-hydroxybutyrate-co-3-hydroxyhexanoate) reinforced with porous cellulose. *ACS Sustain. Chem. Eng.* **2**, 248–253 (2014).
35. Averett, R. D., Realff, M. L. & Jacob, K. I. The effects of fatigue and residual strain on the mechanical behavior of poly(ethylene terephthalate) unreinforced and nanocomposite fibers. *Compos. Part A-Appl. Sci. Manuf.* **40**, 709–723 (2009).
36. Chen, L. et al. Organized assembly of chitosan into mechanically strong bio-composite by introducing a recombinant insect structural protein OfCPH-1. *Carbohydr. Polym.* **334**, 122044 (2024).
37. Shi, S. et al. Remarkably strengthened microinjection molded linear low-density polyethylene (LLDPE) via multi-walled carbon nanotubes derived nanohybrid shish-kebab structure. *Compos. Part B-Eng.* **167**, 362–369 (2019).
38. Si, W.-J., An, X.-P., Zeng, J.-B., Chen, Y.-K. & Wang, Y.-Z. Fully biobased, highly toughened and heat-resistant poly(L-lactide) ternary blends via dynamic vulcanization with poly(D-lactide) and unsaturated bioelastomer. *Sci. China Mater.* **60**, 1008–1022 (2017).
39. Luo, J. et al. Lignin-induced sacrificial conjoined-network enabled strong and tough chitosan membrane for food preservation. *Carbohydr. Polym.* **313**, 120876 (2023).
40. Li, K. et al. Mechanically strong polystyrene nanocomposites by peroxide-induced grafting of styrene monomers within nanoporous cellulose gels. *Carbohydr. Polym.* **199**, 473–481 (2018).
41. Li, J., Zhou, M., Cheng, F., Lin, Y. & Zhu, P. Bioinspired approach to enhance mechanical properties of starch based nacre-mimetic nanocomposite. *Carbohydr. Polym.* **221**, 113–119 (2019).
42. Shao, Y. et al. A tough monolithic-integrated triboelectric bioplastic enabled by dynamic covalent chemistry. *Adv. Mater.* **36**, 2311993 (2024).
43. Chen, G. et al. Scalable, strong and water-stable wood-derived bioplastic. *Chem. Eng. J.* **439**, 135680 (2022).

Acknowledgements

H.Y. acknowledges the support by the National Key Research and Development Program of China (No. 2023YFD2200504) and the National Natural Science Foundation of China (No. 32330072). D.Z. acknowledges the National Natural Science Foundation of China (No. 32171720 and 32371823) and the Liaoning Province Xingliao Talents Leading Talent Program (Grant No. XLYC2402043).

Author contributions

H.Y. and D.Z. supervised the project and designed the experiments. H.T. and S.Z. carried out most of the experiments. Z.T., R.Z., and X.L. participated in the experiments and contributed to the analysis of mechanical and thermal performances. X.L. contributed to the degradability analysis. H.T., S.Z., D.Z., and H.Y. collectively analyzed all data, wrote and revised the paper. All authors discussed the results and commented on the manuscript.

Competing interests

The authors declare no competing interests.

Additional information

Supplementary information The online version contains supplementary material available at https://doi.org/10.1038/s41467-025-63904-2.

Correspondence and requests for materials should be addressed to Suqing Zeng, Dawei Zhao or Haipeng Yu.

Peer review information *Nature Communications* thanks Ren'ai Li, Xiaohui Wang, and the other, anonymous, reviewer(s) for their contribution to the peer review of this work. A peer review file is available.